# Sensitive parameter and its influence law on load sharing performance of double input split torque transmission system

**G. H. Jin[1,2], Y. P. Xiong[2,*], Y. F. Gui[1], R. P. Zhu[1]**

[1] College of Mechanical and Electrical Engineering, Nanjing University of Aeronautics and Astronautics, Nanjing, 210016, China

[2]Faculty of Engineering and the Environment, Fluid Structure Interaction Research Group, University of Southampton, Boldrewood Innovation Campus, SO16 7QF, UK

*Y.Xiong@soton.ac.uk*

**Abstract**

The split-path transmission, particularly attractive alternatives to the traditional epicyclic gear transmission of the helicopter, provides two parallel pathways for transmitting torque from the engine to the rotor. The key technical index of the split path design is to equalize the torque in each path as much as possible. Therefore, it is necessary to study the sensitive design parameters affecting load sharing characteristics. In order to obtain the utmost sensitive parameters and the change law of the effects, a coupled dynamic analysis model considering the time-varying meshing stiffness, mesh errors and mesh damping, is established for the split torque transmission system. Taking support stiffness and torsional stiffness as variables, the sensitivities of load sharing coefficient to these parameters are calculated and analyzed based on sensitive analysis, and the distribution law of the sensitivities of load sharing coefficient is obtained. Results show that load sharing coefficient has a higher sensitivity to the torsional stiffness and the support stiffness of duplicated gear shafts, but lower to input shafts and output shaft. Furthermore, reducing torsional stiffness or increasing two lateral support stiffness of duplicated gear shaft will yield the same results and are contributive to the improvement of load sharing.

**Key words:** Split torque, Dynamic response, Load sharing, Sensitivity, Coupling system

## 1 Introduction

In an effort to satisfy increasingly requirement of user, next generation of helicopters requires drive systems that are lighter, quieter, more reliable and more efficiency, lower noise/vibration than the state of the art [1-2]. Therefore, several scholars have studied the configuration of the drive system of a helicopter, and proposed a novel gear train arrangement known as a split torque or split-path arrangement. A split path design at the final stage of the main gearbox expects to get the advantages of sharing the torque among multiple pinions, as is done in a traditional planetary stage, while also obtaining a larger reduction ratio than is possible for a planetary design. Compared with conventional transmission with a planetary gear stage, White [3-5] has advocated the benefits for a 3600 HP split torque transmission, stating that these designs offer the following advantages over traditional arrangements: (a) large reduction ratio of speed at the final stage, (b) reduced number of reduction stages, (c) increased reliability of the separate drive paths, (e) fewer gears and bearings, (f) lower noise. Obviously, a split torque design is conducive to the realization of the above requirements.

For split torque drivetrains, one of the most important consideration is load sharing. Otherwise, the larger load of one of the two parallel paths will cause tooth fracture. So far, there are some works [6-13] on improving the load sharing performance. One of the most effective methods is the stiffness coordination method. The shaft which has greater flexibility [6, 7, 9] is easier to produce large torsional deformation to counteract the offset load caused by the manufacturing errors, installation errors and structural deformations of the drive system. Although has no additional balance device in the split torque arrangement, the structure of flexible shaft was very complicated, and difficulty to be manufactured and installed. Subsequently, in order to eliminate the special load-sharing devices and achieve load sharing properties in the Comanche and future rotorcraft, Krantz and Delgado [12, 13] proposed another method by introducing the clocking angle of the gear trains considered a design variable of split path gearboxes. Recently, on the basis of careful examination and consideration of the new technologies required for the development of new ch-53k heavy lift helicopter, Yuriy [14-16] et al. provided a detailed transmission configuration of ch-53k helicopter owned three-engine. The split torque technology mentioned in the documents meets the requirements by the use of compliant quill shafts inserted between the second and the third stages. Furthermore, Stamps et al. [17] and Robert et al. [18] expanded split torque design even further and proposed drive system arrangement for

* Corresponding author.

 

the Heavy Lift Civil Tiltrotor.

The stability [19] and the dynamic characteristics [20] of the transmission system have been a focus of attention. Therefore, some scholars also analyzed the dynamic response of split torque transmissions and the factors influencing the load sharing. For example, Krantz et al. [21-22] investigated the vibration and dynamic characteristics of a split path gearbox, and presented the results of studying three variables, shaft angle, mesh stiffness, and compound shaft stiffness. Although Yang et al. [23] and Du et al. [24] have studied nonlinear dynamic characteristics of split torque transmission, the calculation mainly considered the influence of torsional vibration. Zhang et al. [25] obtained the influence law of the error on the load sharing characteristics, and the functional relationship between the error and the meshing load factor. Based on the conditions of deflection compatibility of torsional angle, Dong et al. [26-27] using the statics model analyzed the load sharing coefficient of this system and the influences of the installation and manufacturing errors of each component on the power split. The dynamics model was established by Zhao et al. [28] to study the dynamic behavior of a parallel shaft torque transmission system employing numerical simulation method, and the dynamic load characteristics and the influences of the manufacturing and installation errors on load non-uniform coefficient were analyzed.

As can be seen from the above literatures, the challenges of designing a split drive system are load balance of two paths. Therefore, an effort to discover the important parameters influencing load sharing performance has an important practical significance. For this force closed system, stiffness is a key factor due to the existence of deformation compatibility in the system. The main objective of this paper is to distinguish the utmost sensitive stiffness parameters, and obtain its influential mechanism on load sharing coefficient. Based on the lumped-parameter method, coupled dynamic analysis model taking account of the time-varying meshing stiffness, mesh errors and mesh damping, is established to analyze the dynamic performance using numerical simulation method. Design parameters of the transmission system are determined through an optimization method. Sensitive method is used to obtain the utmost affect weights of stiffness by applying a small perturbation to matrix, and then the change law of load sharing influenced by the stiffness is studied. The research reported here can not only better understand split torque transmissions, but also explore the feasible approach to further improve the load sharing performance.

## 2 Coupled dynamic model of split torque transmission system

### 2.1 Coupled dynamic model

Fig.1 shows arrangement of the split torque transmission in the main gearbox of a helicopter powered by two engines. Among them, the subscript *L* and *R* denote the left input and the right input components respectively. Apparently, this split torque transmission has two power input, and each transfer path is made of split torque stages (Left: the input pinion $Z_{Lp}$ meshes with two gears simultaneously, that is $Z_{L1s}$ and $Z_{L2s}$. Right: similarly, input pinion $Z_{Rp}$ meshes with gear $Z_{R1s}$ and gear $Z_{R2s}$.) and synthesized torque stages (Left: gear $Z_{L1h}$ and gear $Z_{L2h}$. Right: gear $Z_{R1h}$ and gear $Z_{R2h}$. these gears all mesh with output gear $Z_B$ at the same time.). Torque provided by two engines through $Z_{Lp}$ and $Z_{Rp}$, is transferred to engaged two branches of gears respectively, that is $Z_{L1s}$, $Z_{L2s,}$ and $Z_{R1s}$, $Z_{R2s}$. Then, the system realizes the torque split. After that, torque is transmitted to the output gear $Z_B$ through $Z_{R1h}$, $Z_{R2h}$, $Z_{L1h}$ and $Z_{L2h}$, and then torque is integrated. Gear $Z_{R1s}$ and $Z_{R1h}$, gear $Z_{R2s}$ and $Z_{R2h}$, gear $Z_{L1s}$ and $Z_{L1h}$, gear $Z_{L2s}$ and $Z_{L2h}$, are all linked by itself shafts respectively. The angle between two central lines，that is, the center line between $Z_{ji\text{s}}$ and $Z_B$, and another between $Z_{ji\text{s}}$ and $Z_{jp}$, is $\theta_{ji}$. Center lines composed by center point of $Z_{jp}$ and $Z_{j1s}$, and the other by $Z_{jp}$ and $Z_{j2s}$, make up angle $\theta_{jp}$. The lines made of center point of $Z_B$ and $Z_{Rp}$, another line by $Z_B$ and $Z_{Lp}$, create angle $\theta$. Here, $j$=*L*，*R*, and $i$=1，2, as shown in Fig. 2.

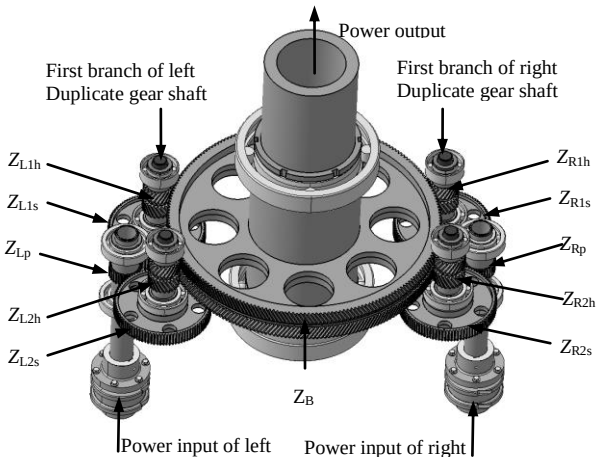


**Fig.1.** Schematic of a double input cylindrical gear split torque system model

The dynamic model shown in Fig.3 contains the rotational inertias of input and output components. *K*, c and e with appropriate subscript represent stiffness, damping and transmission error respectively. The support stiffness of shaft is simulated by spring in the x and y directions. Here, $K_{jpx}$ and $K_{jpy}$, $K_{jix}$ and $K_{jiy}$, $K_{Bx}$ and $K_{By}$, represent support stiffness of input shaft, duplicated gear shaft and output shaft respectively. Shaft is simulated by spring and damping. $K_{jDp}$, $K_{jisih}$ and $K_{Bo}$ represent torsional stiffness of input shaft, duplicated gear shaft and output shaft respectively.

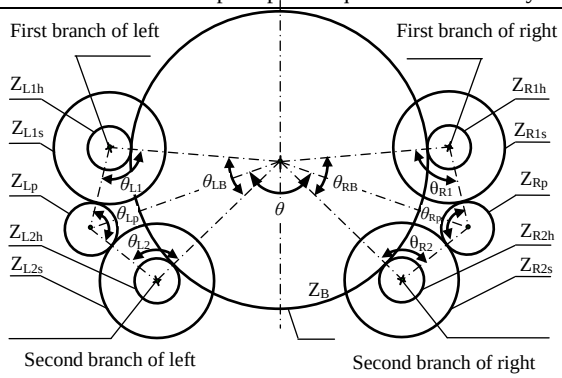


**Fig.2** Installation angle of the split torque transmission system

Therefore, the analytical model shown in Fig.3 can be described using a total of twenty-eight degree of freedom, and then the generalized displacement vector $\bar{\boldsymbol{Y}}$ of the system can be expressed as

$$\begin{aligned}\bar{\boldsymbol{Y}} = \big(&\phi_{\mathrm{Rp}},\phi_{\mathrm{R1s}},\phi_{\mathrm{R2s}},\phi_{\mathrm{R1h}},\phi_{\mathrm{R2h}},\phi_{\mathrm{Lp}},\phi_{\mathrm{L1s}},\phi_{\mathrm{L2s}},\phi_{\mathrm{L1h}},\phi_{\mathrm{L2h}},\phi_{\mathrm{B}},\phi_{\mathrm{RDp}},\phi_{\mathrm{LDp}},\\ &\phi_{\mathrm{o}},X_{\mathrm{Rp}},Y_{\mathrm{Rp}},X_{\mathrm{R1}},Y_{\mathrm{R1}},X_{\mathrm{R2}},Y_{\mathrm{R2}},X_{\mathrm{Lp}},Y_{\mathrm{Lp}},X_{\mathrm{L1}},Y_{\mathrm{L1}},X_{\mathrm{L2}},Y_{\mathrm{L2}},X_{\mathrm{B}},Y_{\mathrm{B}}\big)^{\prime}\end{aligned} \tag{1}$$

where, $\varphi_{jp}$, $\varphi_{jis}$, $\varphi_{jih}$ and $\varphi_{B}$ are angular displacement of gears respectively, these are $Z_{jp}$, $Z_{jis}$, $Z_{jih}$, and $Z_B$. $\varphi_{jDp}$ and $\varphi_o$ represent respectively angular displacement of input and output torsional angles. Displacement in x and y direction of input shaft are $X_{jp}$ and $Y_{jp}$, while output shaft's accordingly are $X_B$ and $Y_B$. Similarly, $X_{ji}$ and $Y_{ji}$ represent displacement of others shafts.

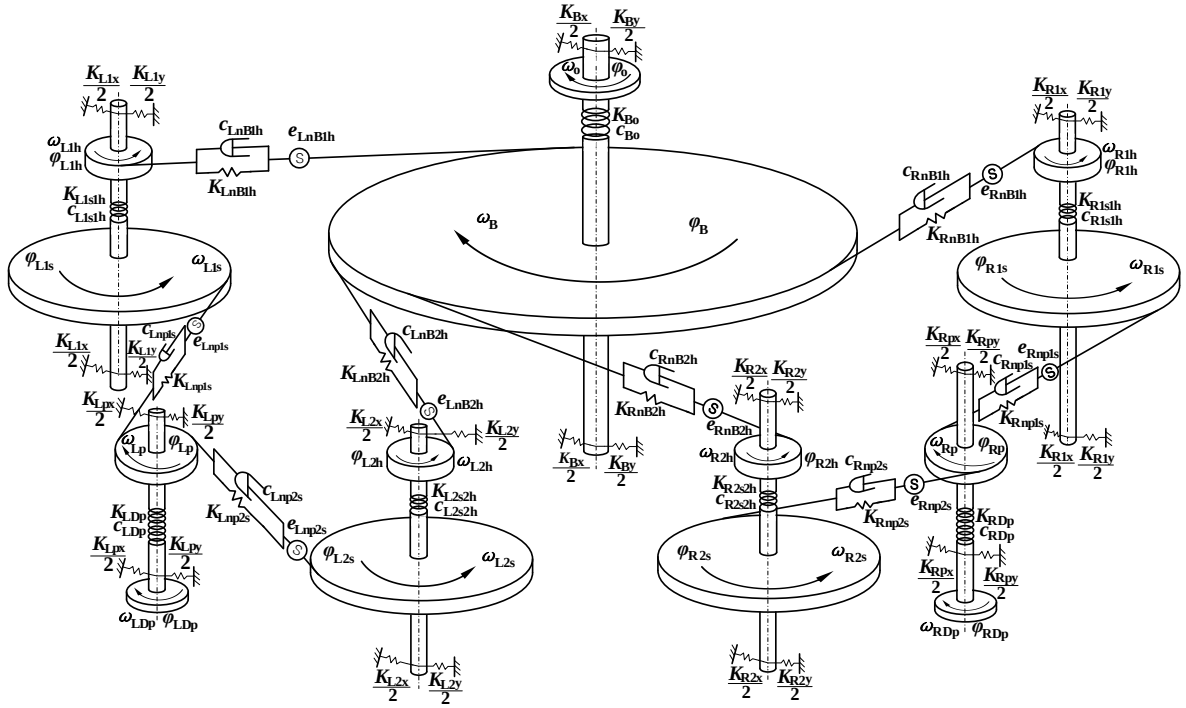

**Fig.3** Dynamic model of cylindrical gear split torque transmission system

### 2.2 Dynamic equations of the system

Fig.4 shows the relationship of local coordinates and global coordinates of the split torque transmission system. Reference coordinate frames with superscript (*) are local, and $Y$ and $Y^*$ in the coordinate systems are parallel to the meshing line of each particular gear pairs. The coordinate of input shaft of two branches is $X_{jp}^*$, $Y_{jp}^*$ and $X_{jp}$, $Y_{jp}$, and the coordinates formed in the coordinate of output gear $Z_B$ are $X_{jB}^*$, $Y_{jB}^*$ and $X_{jB}$, $Y_{jB}$. We hypothesize that $\gamma$ is the transmission angle of corresponding gear pair, means that the sum of the transmission angle and the pressure angle is 90 degrees. Then, transmission angles of two branch of gear pairs are $\gamma_{jnpis}$ and $\gamma_{jnBih}$. By converting the local coordinate via rotational coordinate transformations, the displacements specified in these coordinate frames, which are used for numerical calculation, are described in only the global reference frame. Let $X_B$ instead of $X_{LB}$, and $Y_B$ instead of $Y_{LB}$, then the coordinate transforming of displacement between local coordinates and global coordinates is shown as

$$\begin{cases} \boldsymbol{V}_1^* = \boldsymbol{V}_1 \cos\boldsymbol{\Theta} + \boldsymbol{V}_2 \sin\boldsymbol{\Theta} \\ \boldsymbol{V}_2^* = -\boldsymbol{V}_1 \sin\boldsymbol{\Theta} + \boldsymbol{V}_2 \cos\boldsymbol{\Theta} \end{cases}, \tag{2}$$

where, matrix $V_1^* = [X_{jp}^*, X_{ji}^*, X_{jB}^*, X_{RB}]$, $V_2^* = [Y_{jp}^*, Y_{ji}^*, Y_{jB}^*, Y_{RB}]$, and matrix $\boldsymbol{V}_1 = [X_{jp}, X_{ji}, X_{jB}, X_B]$, $\boldsymbol{V}_2 = [Y_{jp}, Y_{ji}, Y_{jB}, Y_B]$ and $\boldsymbol{\Theta} = [\theta_{jp}, \theta'_{ji}, \theta_{jB}, \theta]$. Vector $\theta'_{R1}$, $\theta'_{R2}$, $\theta'_{L1}$ and $\theta'_{L2}$ are respectively equal to $(\theta_{R1} - \gamma_{RnB1h} - \gamma_{Rnp1s})$, $(\theta_{R2} + \gamma_{RnB2h} + \gamma_{Rnp2s})$, $(\theta_{L1} + \gamma_{LnB1h} + \gamma_{Lnp1s})$ and $(\theta_{L2} - \gamma_{LnB2h} - \gamma_{Lnp2s})$。

According to equilibrium condition of forces, the dynamic equation can be written as

$$\begin{cases} \boldsymbol{I}\ddot{\boldsymbol{\varphi}} + \bar{\boldsymbol{C}}\dot{\boldsymbol{\varphi}} + \bar{\boldsymbol{K}}\boldsymbol{\varphi} = \bar{\boldsymbol{F}} \\ \bar{\boldsymbol{M}}'\ddot{\bar{\boldsymbol{X}}} + \bar{\boldsymbol{K}}'\bar{\boldsymbol{X}} = \bar{\boldsymbol{F}}' \end{cases}, \tag{3}$$

where, $\boldsymbol{I}$ is the inertia matrix of gears, engine and load. Vector $\boldsymbol{\varphi}$ and $\bar{\boldsymbol{F}}$ are angular displacement and generalized force of gear, engine and the load. Matrix $\bar{\boldsymbol{M}}'$, $\bar{\boldsymbol{C}}$, $\bar{\boldsymbol{K}}$ and $\bar{\boldsymbol{K}}'$ denote mass, damping, torsional stiffness and support stiffness of shafts, respectively. Displacement vector and the force vector are $\bar{\boldsymbol{X}}$ and $\bar{\boldsymbol{F}}'$.

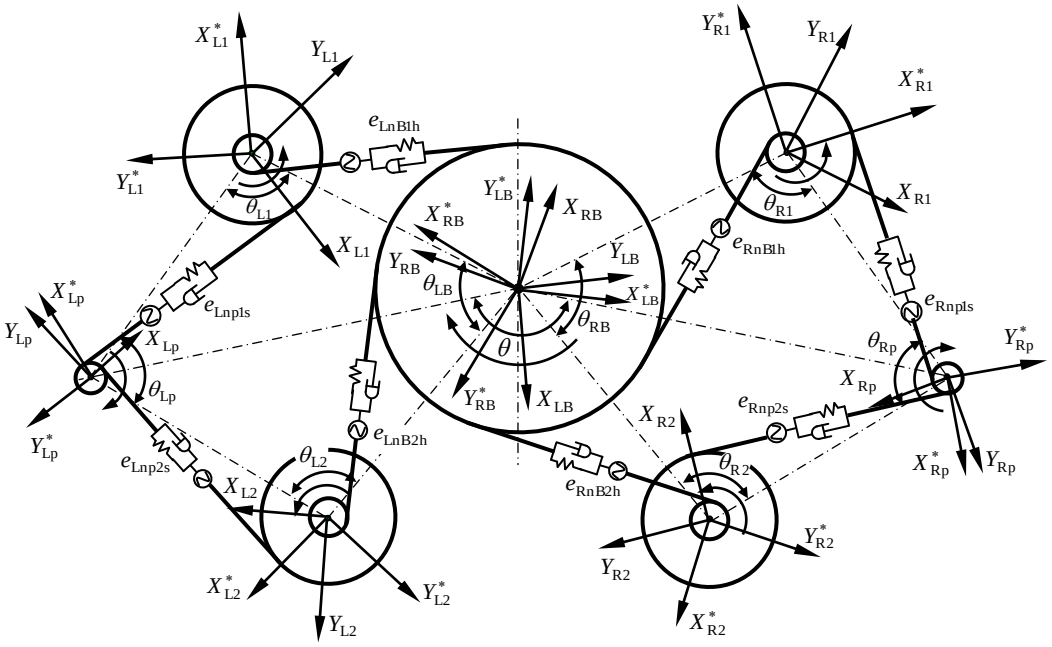


**Fig.4** Relationship of local coordinates and global coordinates

In order to simplify the equation and eliminate the rigid body displacement, the torsional displacements of shafts are converted into a linear displacement, which can be expressed as

$$\begin{cases} Y_{jDp} = r_{jDp}(\phi_{jDp} - \phi_{jp}) \\ Y_{jisih} = r_{jisih}(\phi_{jis} - \phi_{jih}) \\ Y_{Bo} = r_{Bo}(\phi_B - \phi_o) \end{cases}, \tag{4}$$

where, $r_{jDp}$, $r_{jisih}$ and $r_{Bo}$ are respectively the radii of input shaft, duplicate gear shaft and output shaft. According to Fig.3, the torsional displacements of gears can be transformed into the relative displacement along the meshing line of gear pairs. The relative displacement $Y_{jnpis}$ and $Y_{jnBih}$ are expressed as

$$\begin{cases} Y_{Rnp1s} = \left(-Y_{Rp} + r_{Rbp}\phi_{Rp}\right) - \left(Y_{R1}^* + r_{Rb1s}\phi_{R1s}\right) - e_{Rnp1s} \\ Y_{Rnp2s} = \left(-Y_{Rp}^* + r_{Rbp}\phi_{Rp}\right) - \left(Y_{R2} + r_{Rb2s}\phi_{R2s}\right) - e_{Rnp2s} \\ Y_{RnB1h} = \left(-Y_{R1} + r_{Rb1h}\phi_{R1h}\right) - \left(Y_{RB}^* + r_{bB}\phi_B\right) - e_{RnB1h} \\ Y_{RnB2h} = \left(-Y_{R2}^* + r_{Rb2h}\phi_{R2h}\right) - \left(Y_{RB} + r_{bB}\phi_B\right) - e_{RnB2h} \end{cases}, \tag{5a}$$

$$\begin{cases} Y_{\mathrm{Lnp1s}} = \left(-Y_{\mathrm{Lp}}^{*} + r_{\mathrm{Lbp}}\phi_{\mathrm{Lp}}\right) - \left(Y_{\mathrm{L1}} + r_{\mathrm{Lb1s}}\phi_{\mathrm{L1s}}\right) - e_{\mathrm{Lnp1s}} \\ Y_{\mathrm{Lnp2s}} = \left(-Y_{\mathrm{Lp}} + r_{\mathrm{Lbp}}\phi_{\mathrm{Lp}}\right) - \left(Y_{\mathrm{L2}}^{*} + r_{\mathrm{Lb2s}}\phi_{\mathrm{L2s}}\right) - e_{\mathrm{Lnp2s}} \\ Y_{\mathrm{LnB1h}} = \left(-Y_{\mathrm{L1}}^{*} + r_{\mathrm{Lb1h}}\phi_{\mathrm{L1h}}\right) - \left(Y_{\mathrm{LB}} + r_{\mathrm{bB}}\phi_{\mathrm{B}}\right) - e_{\mathrm{LnB1h}} \\ Y_{\mathrm{LnB2h}} = \left(-Y_{\mathrm{L2}} + r_{\mathrm{Lb2h}}\phi_{\mathrm{L2h}}\right) - \left(Y_{\mathrm{LB}}^{*} + r_{\mathrm{bB}}\phi_{\mathrm{B}}\right) - e_{\mathrm{LnB2h}} \end{cases}, \tag{5b}$$

where, $r_{jbp}$, $r_{jbis}$, $r_{jbih}$ and $r_{bB}$ represent the radii of base circle of gears, which are gear $Z_{jp}$, $Z_{jis}$, $Z_{jih}$ and $Z_B$, respectively.

The transmission system is semidefinite and therefore has a rigid body displacement. In order to eliminate the rigid body displacement and solve the dynamic response of the system, it is essential to eliminate two degrees of freedom through the relative displacement $Y_{\mathrm{RnB2h}}$ and $Y_{\mathrm{LnB2h}}$, because they can be represented by other degrees of freedom. So, according to Eq.(4) and Eq.(5), relative displacement $Y_{\mathrm{RnB2h}}$ is given as

$$\begin{aligned} Y_{\mathrm{RnB2h}} = {} & Y_{\mathrm{RnB1h}} + \left(-Y_{\mathrm{R2}}^{*} - Y_{\mathrm{RB}}\right) + \left(-e_{\mathrm{RnB2h}} + e_{\mathrm{RnB1h}}\right) + \left(Y_{\mathrm{R1}} + Y_{\mathrm{RB}}^{*}\right) - \frac{r_{\mathrm{Rb2h}}}{r_{\mathrm{R2s2h}}} Y_{\mathrm{R2s2h}} + \frac{r_{\mathrm{Rb1h}}}{r_{\mathrm{R1s1h}}} Y_{\mathrm{R1s1h}} + \\ & \frac{r_{\mathrm{Rb1h}}}{r_{\mathrm{Rb1s}}}\left(Y_{\mathrm{Rnp1s}} + Y_{\mathrm{Rp}} + Y_{\mathrm{R1}}^{*} + e_{\mathrm{Rnp1s}}\right) - \frac{r_{\mathrm{Rb2h}}}{r_{\mathrm{Rb2s}}}\left(Y_{\mathrm{Rnp2s}} + Y_{\mathrm{Rp}}^{*} + Y_{\mathrm{R2}} + e_{\mathrm{Rnp2s}}\right) \end{aligned}, \tag{6}$$

Similarly, the expression of relative displacement $Y_{\mathrm{LnB2h}}$ can be obtained. Finally, the analytical model can be described using a total of twenty-seven degrees of freedom.

Merging same items of Eqs.(2) - (6), the overall equations of motion without rigid displacement of the split torque transmissions system are constructed systematically as

$$\boldsymbol{M}\ddot{\boldsymbol{Y}} + \boldsymbol{C}\dot{\boldsymbol{Y}} + \boldsymbol{K}\boldsymbol{Y} = \boldsymbol{F}\ , \tag{7}$$

where, $\boldsymbol{M}$ and $\boldsymbol{K}$ are the mass matrix and stiffness matrix respectively, and $\boldsymbol{Y}$ and $\boldsymbol{F}$ are respectively generalized linear displacement vector and generalized force vector.

## 3 Sensitive method for stability and sensitivity analysis

### 3.1 The sensitivity

This paper uses sensitivity to characterize effects of torsional stiffness and support stiffness on load sharing coefficient of this split torque transmission system. Here, sensitivity $S_{Kl}^{\Omega}$ of load sharing coefficient to stiffness variation is defined as [29]

$$S_{K_l}^{\Omega} = \left|\frac{(\Omega' - \Omega)/\Omega}{(K_l' - K_l)/K_l}\right| \times 100\%\ , \tag{8}$$

where, $K_l$ and $K_l'$ express the value of stiffness before and after states, $\Omega$ and $\Omega'$ are the load sharing coefficients corresponding to the before and after states of stiffness, and *l*= *jpx*, *jpy*, *jix*, *jiy*, *jisih*, *jDp*, *Bo*, *Bx* and *By*.

### 3.2 Load sharing coefficient

Using Runge-Kutta numerical integral method of self-adaptive varied steps, dynamic responses of this split torque transmission system are obtained. Thus, substituting dynamic displacement response into Eq.(9) leads to the gear meshing forces $P_{jnpis}$ and $P_{jnBih}$ as follow:

$$\begin{cases} P_{jnpis} = K_{jnpis} Y_{jnpis} \\ P_{jnBih} = K_{jnBih} Y_{jnBih} \end{cases}, \tag{9}$$

where, $K_{jnpis}$ is the meshing stiffness between $Z_{jp}$ and $Z_{jis}$, and $K_{jnBih}$.is the meshing stiffness between $Z_B$ and $Z_{jih}$.

$b_{jisk_1}$ and $b_{jihk_2}$ are respectively load sharing coefficient of split torque stages and synthesized torque stages, which are defined as the ratio of the largest gear meshing force to the average gear meshing force in one tooth period [30].

$$\begin{cases} b_{jisk_1} = \dfrac{N\left(P_{jnpisk_1}\right)_{\max}}{\sum_{i=1}^{N}\left(P_{jnpisk_1}\right)_{\max}} & (k_1 = 1,2,3...n_1) \\ b_{jihk_2} = \dfrac{N\left(P_{jnBihk_2}\right)_{\max}}{\sum_{i=1}^{N}\left(P_{jnBihk_2}\right)_{\max}} & (k_2 = 1,2,3...n_2) \end{cases}, \tag{10}$$

where, $n_1$ and $n_2$ are the number of tooth period of split torque stages and synthesized torque stages respectively, and $N$=2.

$\Omega_{jis}$ and $\Omega_{jih}$, the load sharing coefficient of the system's cycles of each split torque stages and synthesized torque stages, are defined as follow, respectively.

$$\begin{cases} \Omega_{jis} = \left(b_{jisk_1}\right)_{\max} \\ \Omega_{jih} = \left(b_{jihk_2}\right)_{\max} \end{cases}, \tag{11}$$

Further, the load sharing coefficient $\Omega_{js}$ of split torque stages and the load sharing coefficient $\Omega_{jh}$ of synthesized torque stages are described as follow

$$\begin{cases} \Omega_{js} = \left(\Omega_{jis}\right)_{\max} \\ \Omega_{jh} = \left(\Omega_{jih}\right)_{\max} \end{cases}, \tag{12}$$

## 4 Sensitive parameters and its effect on load sharing coefficients

In order to avoid the interference of gear meshing, authors have studied about tooth matching of split torque transmission, and obtained tooth matching formula. Based on the power transmission of general medium helicopter, and taking minimum volume or the least weight as the target, the optimum design parameters of the transmission system are obtained. The basic parameters of double input cylindrical gear split torque transmission are shown in Table 1.

Table 1 Basic parameters of double input split torque transmission system

| Parameter | Value |
|---|---|
| Input power $P$/kW | 1000 |
| Input speed $n$/(r/min) | 10000 |
| Modulus of split torque stages gear $m_{12}$(mm) | 3.5 |
| Modulus of synthesized torque stages gear $m_{34}$(mm) | 3.94 |
| Tooth number of spur gear $Z_{Rp}/Z_{Lp}$ | 31 |
| Tooth number of gear $Z_{R1s}/Z_{L1s}/Z_{R2s}/Z_{L2s}$ | 98 |
| Tooth number of herringbone gear $Z_{R1h}/Z_{L1h}/Z_{R2h}/Z_{L2h}$ | 23 |
| Tooth number of herringbone gear $Z_B$ | 215 |
| Pressure angle of split torque stages gear $\alpha_{12}$/(°) | 22.5 |
| Pressure angle of synthesized torque stages gear $\alpha_{34}$/(°) | 20 |
| Helical angle of synthesized torque stages gear $\beta_{34}$ /(°) | 30 |
| Tooth width of split torque stages gear $b_{12}$/(mm) | 48 |
| Tooth width of synthesized torque stages gear $b_{34}$/(mm) | 120 |
| Installation angle $\theta_{R1}/\theta_{R2}/\theta_{L1}/\theta_{L2}$/(°) | 108.5 |
| Installation angle $\theta_{RP}/\theta_{LP}$/(°) | 104.5 |
| Installation angle $\theta$/(°) | 180 |

### 4.1 Sensitivity analysis of support stiffness on the load sharing coefficient

（1）Sensitivity calculation and analysis

There are many support stiffness in the split torque transmission system. The variations of sensitivities of load sharing coefficient to these support stiffness whose numerical value are applied 7.5% perturbations are respectively shown in Fig.5 and Fig.6. The numbers 1 to 14 of horizontal axis represent respectively the support stiffness designated by $K_{Rpx}$, $K_{Rpy}$, $K_{R1x}$, $K_{R1y}$, $K_{R2x}$, $K_{R2y}$, $K_{Lpx}$, $K_{Lpy}$, $K_{L1x}$, $K_{L1y}$, $K_{L2x}$, $K_{L2y}$, $K_{Bx}$ and $K_{By}$.

It can be seen from Fig.5 and Fig.6 that the sensitivity of the support stiffness to load sharing coefficients varies greatly, and the sensitivity is mainly affected by the support stiffness of its drive subsystem. The results show that the load sharing coefficient is very sensitive to the support stiffness $K_{L1x}$, $K_{R1y}$, $K_{R2x}$ and $K_{L2y}$. The load sharing coefficient of right split torque stages is extremely sensitive to the support stiffness $K_{R2x}$ as shown in Fig.5 (a) and Fig.5 (b). And the load sharing coefficient of synthesized torque stages is more sensitive to the support stiffness $K_{R1y}$ as shown in Fig.5(c) and Fig.5 (d). For the transmission system of the left branch, the support stiffness $K_{L1x}$ mainly influences the sensitivity of load sharing coefficient of split torque stages, as shown in Fig.6 (a) and Fig. 6(b), and the support stiffness $K_{L2y}$ mainly influences the sensitivity of synthesized torque stages, as shown in Fig.6 (c) and Fig.6 (d).

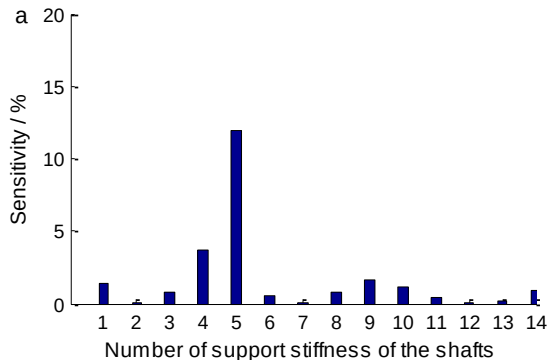


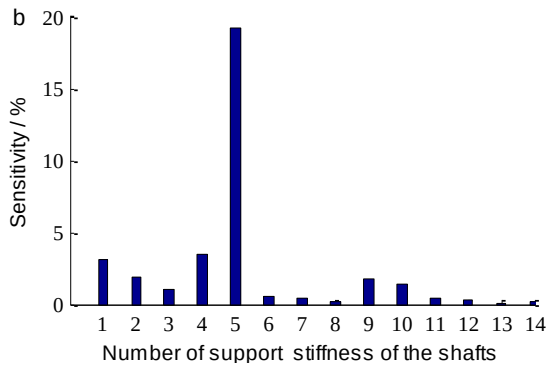

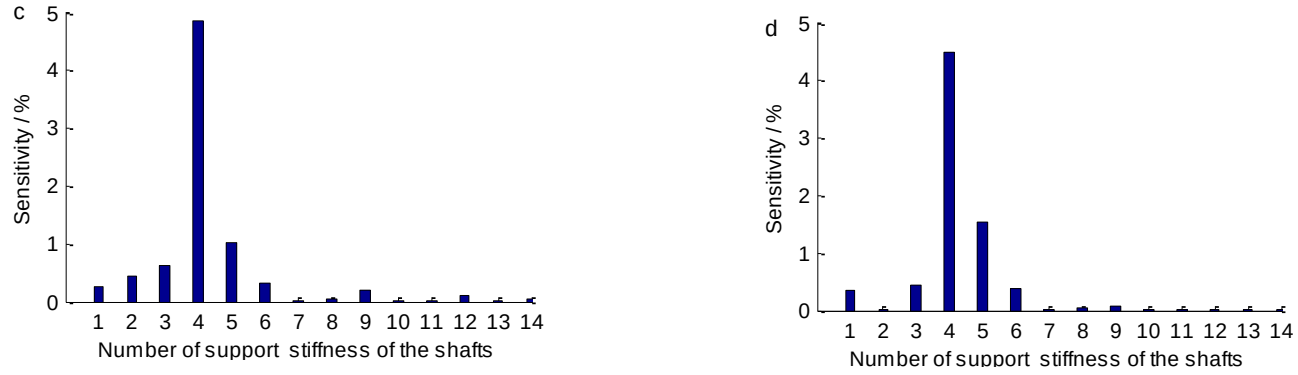


**Fig.5** Effect of support stiffness of right input on sensitivity of load sharing. (a) $S_{K_l}^{\Omega_{\mathrm{R1s}}}$, (b) $S_{K_l}^{\Omega_{\mathrm{R2s}}}$, (c) $S_{K_l}^{\Omega_{\mathrm{R1h}}}$, (d) $S_{K_l}^{\Omega_{\mathrm{R2h}}}$.

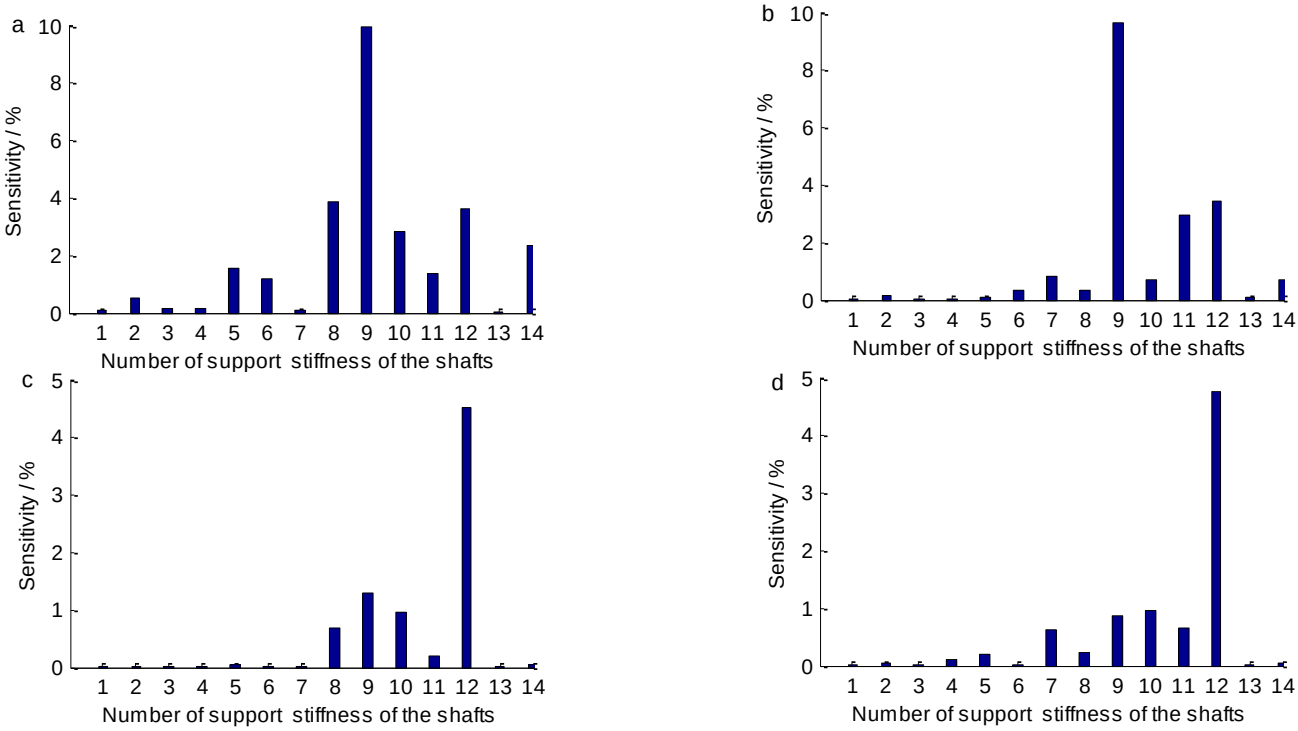


**Fig.6** Effect of support stiffness of left input on sensitivity of load sharing. (a) $S_{K_l}^{\Omega_{\mathrm{L1s}}}$, (b) $S_{K_l}^{\Omega_{\mathrm{L2s}}}$, (c) $S_{K_l}^{\Omega_{\mathrm{L1h}}}$, (d) $S_{K_l}^{\Omega_{\mathrm{L2h}}}$.

As can be seen from Fig.1 that the transmission system has the characteristics of force closure, and the geometry of the transmission subsystem is similar. However, although the geometrical structure is similar, the meshing forces between the gear pairs are not symmetrical. Therefore, the deformation and sensitivity in the direction of the supporting stiffness are also different. The deformation of the support structure results in a change in the center distance of gear pair. The change of center distance will lead to the change of the gear's deflection angle, and then the degree of variation of load sharing coefficient will be different. Hence, in the structural design of the transmission system, the stiffness of the support should be properly optimized.

（2）Sensitive support stiffness influence on load sharing coefficients

To further study the relationship between the sensitive support stiffness and the load sharing coefficients, the influences of support stiffness designated by $K_{\mathrm{R1}y}$ and $K_{\mathrm{L2}y}$ on load sharing coefficients are analyzed in the case of that other parameters remain unchanged, as shown in Fig.7. The following conclusions may be drawn from the analysis results. The Fig.7 shows that the load sharing coefficients of the split torque stages and the synthesized torque stages of right branch both become better with the increase of support stiffness $K_{\mathrm{R1}y}$, and the load sharing coefficients of the split torque stages and the synthesized torque stages of left branch are gradually close to 1 with the increase of support stiffness $K_{\mathrm{L2}y}$, but the support stiffness $K_{\mathrm{R1}y}$ and $K_{\mathrm{L2}y}$ almost do not affect the load sharing performance of subsystem of the other side. The load sharing coefficients of the split torque stages and the synthesized torque stages of the two branches decrease as the support stiffness

$K_{R1y}$ and $K_{L2y}$ both increase simultaneously, as shown in Fig.7(c). Further analyses show that vibration centerline of the shaft center for the input stages is close to each other and the difference of the deflection angle of input stages decreases, as a result, the load sharing performance of the system is improved.

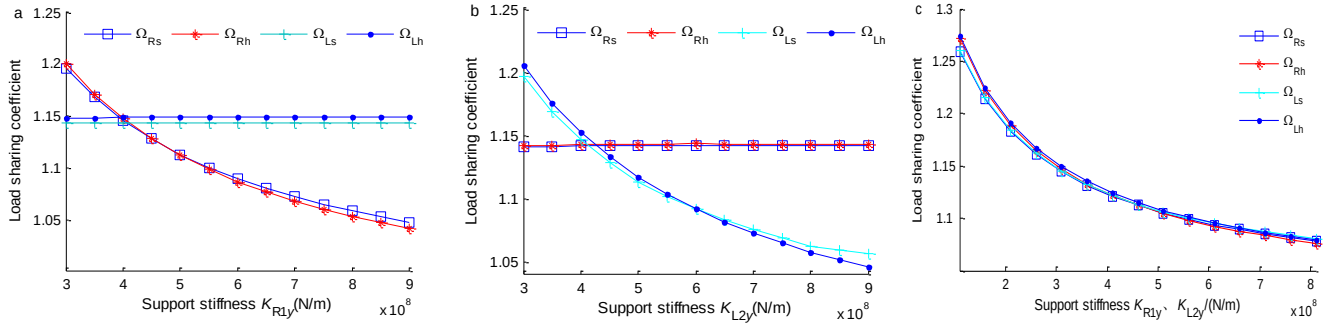


**Fig.7** Influential mechanism of support stiffness $K_{R1y}$ and $K_{L2y}$ on load sharing coefficient.
(a) Stiffness of $K_{R1y}$ changes, (b) Stiffness of $K_{L2y}$ changes, (c) Stiffness of $K_{R1y}$ and $K_{L2y}$ both change.

Load sharing performances become worse with the increase of the support stiffness designated by $K_{R2x}$ and $K_{L1x}$ in the case of that the other parameters remain unchanged, as shown in Fig.8. Increasing the support stiffness $K_{R2x}$ and $K_{L1x}$ respectively, the load sharing coefficient of the split torque stages and the synthesized torque stages of the corresponding branch increases and is gradually far away from 1, but the load sharing performance of the subsystem of the other side is almost not affected, as shown in Fig.8 (a) and Fig.8 (b). When both the support stiffness $K_{R2x}$ and $K_{L1x}$ increases simultaneously, load sharing performance of the system deteriorates as shown in Fig.8(c).

The further study shows that although the geometry of the system is symmetrical, and the torsional stiffness and support stiffness of the shaft are equal, the influences of the support stiffness $K_{R1y}$, $K_{R2x}$, $K_{L1x}$ and $K_{L2y}$ on the load sharing coefficients are apparent. This is because that the manufacturing error, installation error and structural deformation will make the force of the gear train be asymmetrical, and then the gear center will produce lateral micro-displacement, with the result of that, the rotational deformation of the gears are different and the power of the two branches is out of balance. Hence, an appropriate improve the stiffness value in the direction is a wise choice in the design.

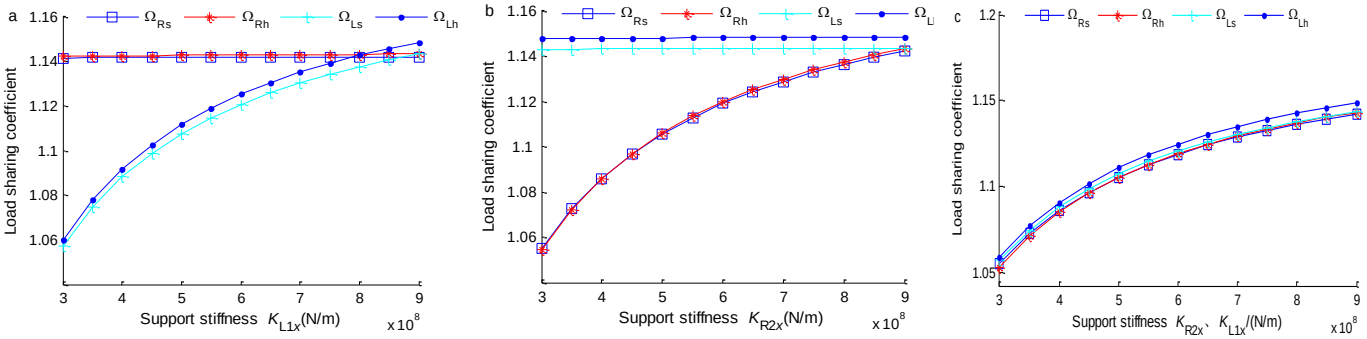


**Fig.8** Influential mechanism of support stiffness $K_{L1x}$ and $K_{R2x}$ on load sharing coefficient.
(a) Stiffness of $K_{L1x}$ changes, (b) Stiffness of $K_{R2x}$ changes, (c) Stiffness of $K_{L1x}$ and $K_{R2x}$ both change.

### 4.2 Sensitivity analysis of torsional stiffness on the load sharing coefficient

（1）Sensitivity calculation and analysis

There are seven shafts in this double input split torque transmission system. The variations of sensitivities of load sharing coefficient relation to the torsional stiffness are respectively shown in Fig.9 and Fig.10, in which the changed method of torsional stiffness value is the same as support stiffness.

The numbers 1 to 7 of horizontal axis represent respectively the torsional stiffness designated by $K_{RDp}$, $K_{R1s1h}$, $K_{R2s2h}$, $K_{LDp}$, $K_{L1s1h}$, $K_{L2s2h}$ and $K_{Bo}$. The results show that the sensitivity to its own torsional stiffness of duplicate gear shaft is the highest, so the torsional stiffness of duplicate gear shaft is very important for the system to implement load share. If the flexibility of duplicate gear shaft increases, the duplicate gear shaft is easier to produce large torsional deformation to counteract the offset load caused by the manufacturing errors, installation errors and structural deformations of the drive system, as a result, the load sharing characteristics will be improved. This influence trend and the importance of duplicate gear shaft on the load

sharing are similar with the results in [9].

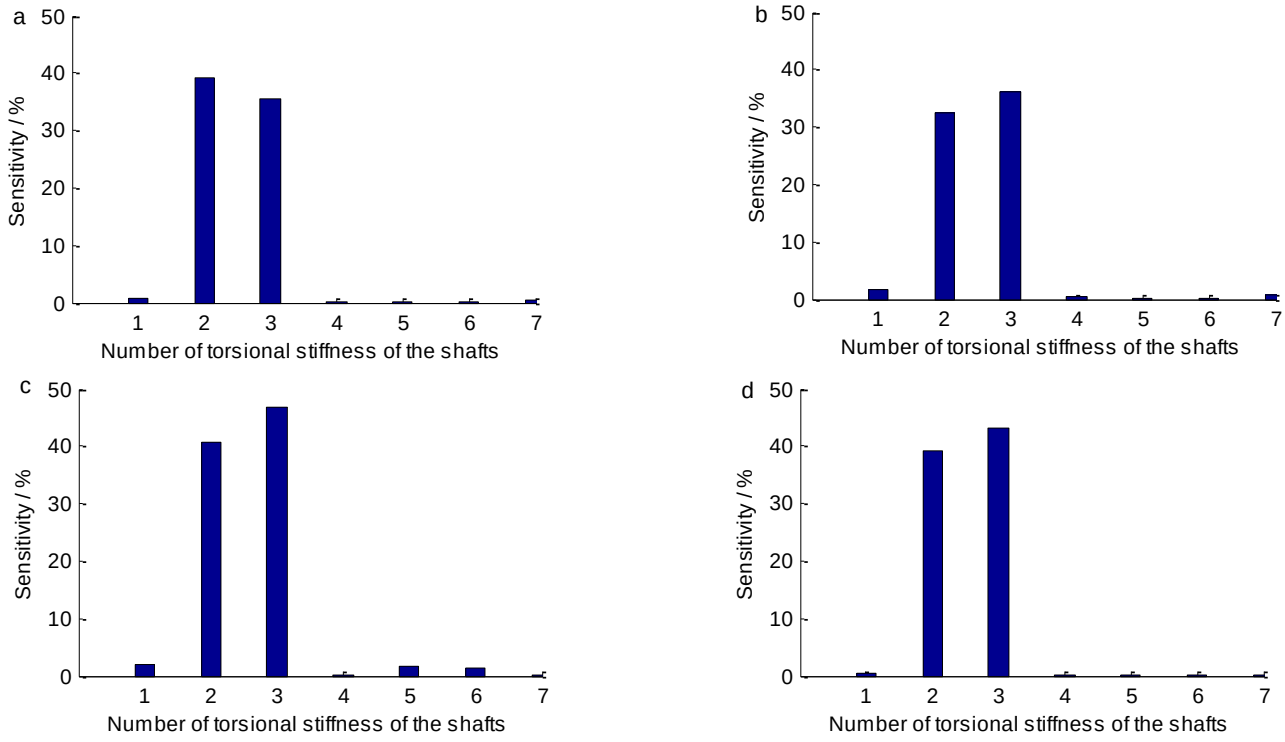


**Fig.9** Effect of torsional stiffness of right input on sensitivity of load sharing. (a) $S_{K_l}^{\Omega_{\mathrm{R1s}}}$, (b) $S_{K_l}^{\Omega_{\mathrm{R2s}}}$, (c) $S_{K_l}^{\Omega_{\mathrm{R1h}}}$, (d) $S_{K_l}^{\Omega_{\mathrm{R2h}}}$.

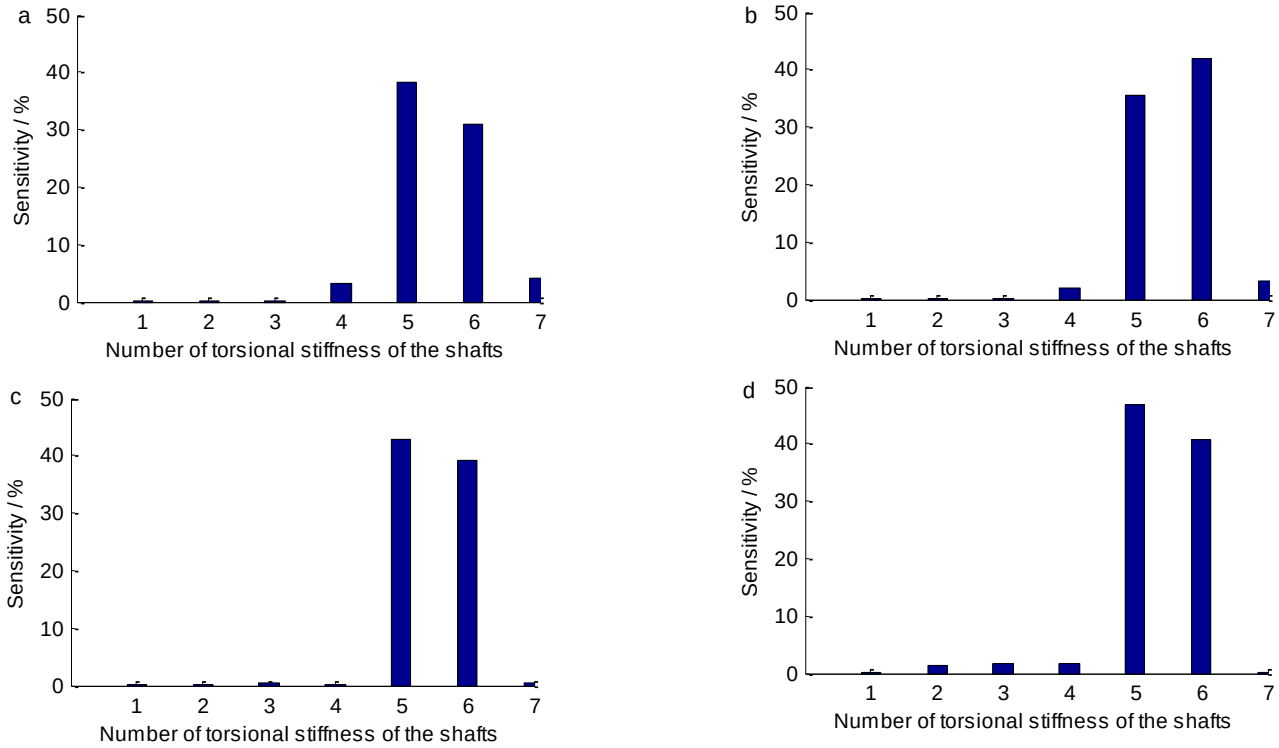


**Fig.10** Effect of torsional stiffness of left input on sensitivity of load sharing. (a) $S_{K_l}^{\Omega_{\mathrm{L1s}}}$, (b) $S_{K_l}^{\Omega_{\mathrm{L2s}}}$, (c) $S_{K_l}^{\Omega_{\mathrm{L1h}}}$, (d) $S_{K_l}^{\Omega_{\mathrm{L2h}}}$.

（2）Sensitive torsional stiffness influence on load sharing coefficients

In order to further study the relationship between the torsional stiffness and the load sharing coefficients, the influence of torsional stiffness of duplicate gear shaft on the load sharing coefficients is analyzed in the case of other parameters remain unchanged, as shown in Fig.11. The load sharing coefficients will deteriorate with the increase of torsional stiffness of duplicate gear shaft. The main reason can be summarized as follow: the proportion of rotational deformation of gear caused by the lateral micro-displacement of gear center in the factors of non-uniform load increases gradually with the increase of

torsional stiffness, but the proportion of torsional deformation of duplicate gear shaft decreases gradually. The torsional stiffness of output gear shaft is large, so the change of amplitude of load sharing coefficient of synthesized torque stages is small, but split torque stages' is big, as shown in Fig.12. Obviously, the load sharing characteristics of split torque stages are the main impact factor of the dynamic performance.

To improve load sharing performance of system, the torsional stiffness of duplicate gear shaft is needed to be minimized. It can be implemented by an inserted elastic torsional shaft to obtain a smaller torsional stiffness so as to improve load sharing performance. Therefore, the design technology of matching the strength and stiffness of duplicate gear shaft needs to be studied in order to ensure the realization of load sharing coefficient.

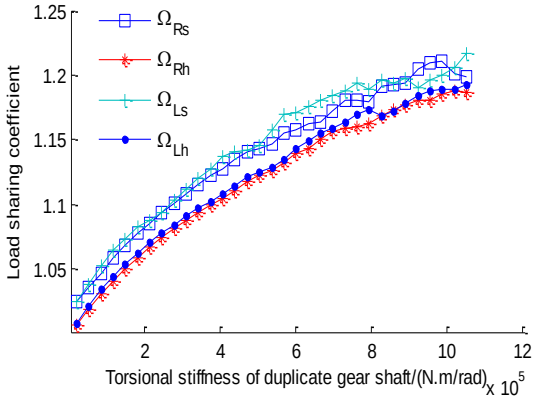


**Fig.11** Influential mechanism of torsional stiffness of duplicate gear shafts on load sharing coefficient

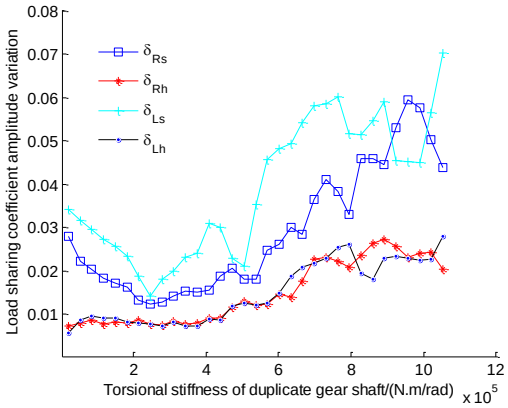


**Fig.12** Effect of torsional stiffness on changed amplitude of load sharing coefficient

## 5 Conclusions

A detailed analysis of the utmost sensitive stiffness parameters affecting load sharing performance and the influence law of the most sensitive parameters are presented in this paper. Though very simple, this analysis emphasizes the sensitive stiffness and its influence law on load sharing of the system. Otherwise, the prediction of the main factors affecting the performance of load sharing may become less effective, as there is a lot of stiffness in the transmission system. The following results are obtained according to the calculation and analysis.

(Ⅰ) Load sharing coefficient is sensitive to the support stiffness designated by $K_{R2x}$, $K_{L1x}$, $K_{R1y}$ and $K_{L2y}$. The increase of support stiffness $K_{R2x}$ and $K_{L1x}$ is not conducive to improve load sharing performance of the drive system, but a suitable increase of support stiffness $K_{R1y}$ and $K_{L2y}$ has the opposite effect compared with support stiffness $K_{R2x}$ and $K_{L1x}$.

(Ⅱ) Load sharing coefficient is sensitive to all but its own torsional stiffness of duplicate gear shaft, and the load sharing coefficient will deteriorate with the increase of torsional stiffness of duplicate gear shaft.

(Ⅲ) On the premise of strength and dynamic stability assurance, the torsional stiffness of duplicate gear shaft is needed to be minimized so as to improve the load sharing performance of the drive system. So, a more detailed analysis on matching design technology of the strength and stiffness of duplicate gear shaft and the structure design of large gear of the duplicate gear are necessary.

(Ⅳ) It is very useful to distinguish the utmost sensitive installation and manufacture errors by using this method. Therefore, how to configure reasonably the installation and manufacture errors is another important duty.

(Ⅴ) In order to further improve the dynamic performance of split torque transmission system, appropriate matching design of spline pair featuring low torsional stiffness and suitable phase relationship between teeth coordinating errors, are beneficial to improve the loading sharing coefficient.

## 6 Acknowledgments

The authors are very grateful to editors and anonymous reviewers for their constructive comments. Those comments are all valuable and very helpful for revising and improving our paper, as well as the important guiding significance to our researches. The authors gratefully acknowledge the financial support by National Natural Science Foundation of China (Grant No. 51475226) and the China Scholarship Council (CSC). Meanwhile, the author wishes to express sincere gratitude

to the Fluid Structure Interactions Research Group of the University of Southampton for providing excellent working conditions and the academic atmosphere.

## Appendix

Eq. (7) can be expressed as

$$\begin{cases} \ddot{Y}_{\mathrm{Rnp1s}}+\dfrac{F_{\mathrm{Rp}y}-K_{\mathrm{Rp}y}Y_{\mathrm{Rp}}}{m_{\mathrm{Rp}}}-\dfrac{F_{\mathrm{R1}x}-K_{\mathrm{R1}x}X_{\mathrm{R1}}}{M_{\mathrm{R1}}}\sin\theta'_{\mathrm{R1}}+\dfrac{F_{\mathrm{R1}y}-K_{\mathrm{R1}y}Y_{\mathrm{R1}}}{M_{\mathrm{R1}}}\cos\theta'_{\mathrm{R1}}- \\ \quad P_{\mathrm{RDp}}\dfrac{r_{\mathrm{Rbp}}}{r_{\mathrm{RDp}}I_{\mathrm{Rp}}}+\left(F_{\mathrm{Rnp1s}}+F_{\mathrm{Rnp2s}}\right)\dfrac{r_{\mathrm{Rbp}}^2}{I_{\mathrm{Rp}}}+F_{\mathrm{Rnp1s}}\dfrac{r_{\mathrm{Rb1s}}^2}{I_{\mathrm{R1s}}}-P_{\mathrm{R1s1h}}\dfrac{r_{\mathrm{Rb1s}}}{r_{\mathrm{R1s1h}}I_{\mathrm{R1s}}}+\ddot{e}_{\mathrm{Rnp1s}}=0 \\ \ddot{Y}_{\mathrm{Rnp2s}}+\dfrac{F_{\mathrm{R2}y}-K_{\mathrm{R2}y}Y_{\mathrm{R2}}}{M_{\mathrm{R2}}}-\dfrac{F_{\mathrm{Rp}x}-K_{\mathrm{Rp}x}X_{\mathrm{Rp}}}{m_{\mathrm{Rp}}}\sin\theta_{\mathrm{Rp}}+\dfrac{F_{\mathrm{Rp}y}-K_{\mathrm{Rp}y}Y_{\mathrm{Rp}}}{m_{\mathrm{Rp}}}\cos\theta_{\mathrm{Rp}}- \\ \quad P_{\mathrm{RDp}}\dfrac{r_{\mathrm{Rbp}}}{r_{\mathrm{RDp}}I_{\mathrm{Rp}}}+\left(F_{\mathrm{Rnp1s}}+F_{\mathrm{Rnp2s}}\right)\dfrac{r_{\mathrm{Rbp}}^2}{I_{\mathrm{Rp}}}+F_{\mathrm{Rnp2s}}\dfrac{r_{\mathrm{Rb2s}}^2}{I_{\mathrm{R2s}}}-P_{\mathrm{R2s2h}}\dfrac{r_{\mathrm{Rb2s}}}{r_{\mathrm{2s2h}}I_{\mathrm{R2s}}}+\ddot{e}_{\mathrm{Rnp2s}}=0 \\ \ddot{Y}_{\mathrm{RnB1h}}+\left(-\sin\theta_{\mathrm{RB}}\cos\theta-\cos\theta_{\mathrm{RB}}\sin\theta\right)\dfrac{F_{\mathrm{B}x}-K_{\mathrm{B}x}X_{\mathrm{B}}}{m_{\mathrm{B}}}+\left(-\sin\theta_{\mathrm{RB}}\sin\theta+\cos\theta_{\mathrm{RB}}\cos\theta\right)\dfrac{F_{\mathrm{B}y}-K_{\mathrm{B}y}Y_{\mathrm{B}}}{m_{\mathrm{B}}}+ \\ \quad \dfrac{F_{\mathrm{R1}y}-K_{\mathrm{R1}y}Y_{\mathrm{R1}}}{M_{\mathrm{R1}}}-P_{\mathrm{R1s1h}}\dfrac{r_{\mathrm{Rb1h}}}{r_{\mathrm{R1s1h}}I_{\mathrm{R1h}}}+F_{\mathrm{RnB1h}}\dfrac{r_{\mathrm{Rb1h}}^2}{I_{\mathrm{R1h}}}+\left(F_{\mathrm{RnB1h}}+F_{\mathrm{RnB2h}}+F_{\mathrm{LnB1h}}+F_{\mathrm{LnB2h}}\right)\dfrac{r_{\mathrm{bB}}^2}{I_{\mathrm{B}}}-P_{\mathrm{Bo}}\dfrac{r_{\mathrm{bB}}}{r_{\mathrm{Bo}}I_{\mathrm{B}}}+\ddot{e}_{\mathrm{RnB1h}}=0 \end{cases} \tag{13}$$

where, $M_{Ri}=m_{Ris}+m_{Rih}$, $P_{jDp}=K_{jDp}Y_{jDp}+c_{jDp}\dot{Y}_{jDp}$, $P_{\mathrm{Bo}}=K_{\mathrm{Bo}}Y_{\mathrm{Bo}}+c_{\mathrm{Bo}}\dot{Y}_{\mathrm{Bo}}$.

$$\begin{cases} \ddot{Y}_{RDp}-T_{RD}\dfrac{r_{RDp}}{I_{RD}}+P_{RDp}\left(\dfrac{1}{I_{RD}}+\dfrac{1}{I_{\mathrm{Rp}}}\right)-\left(F_{Rnp1s}+F_{Rnp2s}\right)\dfrac{r_{Rbp}r_{RDp}}{I_{Rp}}=0 \\ \ddot{Y}_{R1s1h}-F_{Rnp1s}\dfrac{r_{Rb1s}r_{R1s1h}}{I_{R1s}}+P_{R1s1h}\left(\dfrac{1}{I_{R1s}}+\dfrac{1}{I_{R1h}}\right)-F_{RnB1h}\dfrac{r_{Rb1h}r_{R1s1h}}{I_{R1h}}=0 \\ \ddot{Y}_{R2s2h}-F_{Rnp2s}\dfrac{r_{Rb2s}r_{R2s2h}}{I_{R2s}}+P_{R2s2h}\left(\dfrac{1}{I_{R2s}}+\dfrac{1}{I_{R2h}}\right)-F_{RnB2h}\dfrac{r_{Rb2h}r_{R2s2h}}{I_{R2h}}=0 \\ \ddot{Y}_{Bo}-\left(F_{RnB1h}+F_{RnB2h}+F_{LnB1h}+F_{LnB2h}\right)\dfrac{r_{bB}r_{Bo}}{I_B}+P_{Bo}\left(\dfrac{1}{I_B}+\dfrac{1}{I_o}\right)-\dfrac{T_o r_{Bo}}{I_o}=0 \end{cases} \tag{14}$$

where, $P_{jisih}=K_{jisih}Y_{jisih}+c_{jisih}\dot{Y}_{jisih}$.

$$\begin{cases} \ddot{Y}_{Lnp1s}+\dfrac{F_{L1y}-K_{L1y}Y_{L1}}{M_{L1}}-\dfrac{F_{Lpx}-K_{Lpx}X_{Lp}}{m_{Lp}}\sin\theta_{Lp}+\dfrac{F_{Lpy}-K_{Lpy}Y_{Lp}}{m_{Lp}}\cos\theta_{Lp}- \\ \quad P_{LDp}\dfrac{r_{Lbp}}{r_{LDp}I_{Lp}}+(F_{Lnp1s}+F_{Lnp2s})\dfrac{r_{Lbp}^2}{I_{Lp}}+F_{Lnp1s}\dfrac{r_{Lb1s}^2}{I_{L1s}}-P_{L1s1h}\dfrac{r_{Lb1s}}{r_{L1s1h}I_{L1s}}+\ddot{e}_{Lnp1s}=0 \\ \ddot{Y}_{Lnp2s}+\dfrac{F_{Lpy}-K_{Lpy}Y_{Lp}}{m_{Lp}}-\dfrac{F_{L2x}-K_{L2x}X_{L2}}{M_{L2}}\sin\theta'_{L2}+\dfrac{F_{L2y}-K_{L2y}Y_{L2}}{M_{L2}}\cos\theta'_{L2}-P_{LDp}\dfrac{r_{Lbp}}{r_{LDp}I_{Lp}}+ \\ \quad (F_{Lnp1s}+F_{Lnp2s})\dfrac{r_{Lbp}^2}{I_{Lp}}+F_{Lnp2s}\dfrac{r_{Lb2s}^2}{I_{L2s}}-P_{L1s1h}\dfrac{r_{Lb2s}}{r_{L2s2h}I_{L2s}}+\ddot{e}_{Lnp2s}=0 \\ \ddot{Y}_{LnB1h}+\dfrac{F_{By}-K_{By}Y_B}{m_B}-\dfrac{F_{L1x}-K_{L1x}X_{L1}}{M_{L1}}\sin\theta_{L1}+\dfrac{F_{L1y}-K_{L1y}Y_{L1}}{M_{L1}}\cos\theta_{L1}-P_{L1s1h}\dfrac{r_{Lb1h}}{r_{L1s1h}I_{L1h}}- \\ \quad F_{LnB1h}\dfrac{r_{Lb1h}^2}{I_{L1h}}+(F_{RnB1h}+F_{RnB2h}+F_{LnB1h}+F_{LnB2h})\dfrac{r_{bB}^2}{I_B}-P_{Bo}\dfrac{r_{bB}}{r_{Bo}I_B}+\ddot{e}_{LnB1h}=0 \end{cases} \tag{15}$$

where, $M_{L1}$ and $M_{L2}$ are respectively equal to ($m_{L1s}$+$m_{L1h}$) and ($m_{L2s}$+$m_{L2h}$).

$$\begin{cases} \ddot{Y}_{LDp}-T_{LD}\dfrac{r_{LDp}}{I_{LD}}+P_{LDp}\left(\dfrac{1}{I_{LD}}+\dfrac{1}{I_{\mathrm{Lp}}}\right)-\left(F_{Lnp1s}+F_{Lnp2s}\right)\dfrac{r_{Lbp}r_{LDp}}{I_{Lp}}=0 \\ \ddot{Y}_{L1s1h}-F_{Lnp1s}\dfrac{r_{Lb1s}r_{L1s1h}}{I_{L1s}}+P_{L1s1h}\left(\dfrac{1}{I_{L1s}}+\dfrac{1}{I_{L1h}}\right)-F_{LnB1h}\dfrac{r_{Lb1h}r_{L1s1h}}{I_{L1h}}=0 \\ \ddot{Y}_{L2s2h}-F_{Lnp2s}\dfrac{r_{Lb2s}r_{L2s2h}}{I_{L2s}}+P_{L2s2h}\left(\dfrac{1}{I_{L2s}}+\dfrac{1}{I_{L2h}}\right)-F_{LnB2h}\dfrac{r_{Lb2h}r_{L2s2h}}{I_{L2h}}=0 \end{cases} \tag{16}$$

$$\begin{cases} m_{jp}\ddot{X}_{jp} + K_{jpx}X_{jp} - F_{jpx} = 0 \\ m_{jp}\ddot{Y}_{jp} + K_{jpy}Y_{jp} - F_{jpy} = 0 \\ M_{ji}\ddot{X}_{ji} + K_{jix}X_{ji} - F_{jix} = 0 \\ M_{ji}\ddot{Y}_{ji} + K_{jiy}Y_{ji} - F_{jiy} = 0 \\ m_B\ddot{X}_B + K_{Bx}X_B - F_{Bx} = 0 \\ m_B\ddot{Y}_B + K_{By}Y_B - F_{By} = 0 \end{cases} \tag{17}$$

## References


[1] John J. Coy and Robert C. Bill, Advanced transmission studies, *NASA Technical Memorandum 100867*, pp. 1-14, 1988.

[2] R. B. Bossler Jr and G. F. Heath, Advanced rotorcraft transmission program summary, *In*: *AIAA/SAE/ASME/ASEE 28th Joint Propulsion Conference and Exhibit*, pp. 1-12, 1992.

[3] White G., New family of high-ratio reduction gear with multiple drive paths, *Proc Inst Mech Eng*, vol. 188, pp. 281-288, 1974.

[4] White G., Design study of a 375 kW helicopter transmission with split-torque epicyclic and bevel drive stages, *Proc Inst Mech Eng C J Mech Eng Sci*, vol. 197, pp. 213-224, 1983.

[5] White G., Split torque helicopter transmissions with widely separated engines, *Proc Inst Mech Eng G J Aerosp Eng*, vol. 203, pp. 53-65, 1989.

[6] Cocking, H., The design of an advanced engineering gearbox, *Vertica*, vol. 10, pp. 213-225, 1986.

[7] Smirnov G., Multiple-power-path nonplanetary main gearbox of the Mi-26 heavy-lift transport helicopter, *Vertiflite*, vol. 36, pp. 20-23, 1990.

[8] Kish J. G., Sikorsky aircraft advanced rotorcraft transmission (ART) program-final report, *NASA Contractor Report 191079*, pp. 1-212, 1993.

[9] White G., Design study of a split-torque helicopter transmission. *Proc Inst Mech Eng G J Aerosp Eng*, vol. 212, pp. 117-123, 1998.

[10] Majid Rashidi and Timothy Krantz, Dynamics of a split torque helicopter transmission, *NASA Technical Memorandum 105681*, pp. 1-12, 1992.

[11] Krantz T. L., Dynamics of a split torque helicopter transmission, *NASA Technical Memorandum 106410*, pp. 1-43, 1994.

[12] Krantz T. L., A method to analyze and optimize the load sharing of split path transmissions, *NASA Technical Memorandum 107201*, pp. 1-21, 1996.

[13] Krantz T. L., Delgado I. R., Experimental study of split-path transmission load sharing, *NASA Technical Memorandum 107202*, pp. 1-11, 1996.

[14] Yuriy Gmirya and Shulin He, Gregory Buzel, Leslie Leigh, Load sharing test of the CH-53K split torque main gearbox, *In: the American Helicopter Society 65th Annual Forum*, pp. 977-986, 2009.

[15] Yuriy Gmirya and Woodbridge, Multi-path rotary wing aircraft gearbox, *United States Patent US 7918146B2*, Apr 5, 2011.

[16] Yuriy Gmirya, Matthew Alulis, Peter palcic and Leslie Leigh, Design and development of a modern transmission: baseline configuration of the CH-53K drive system. *In: the American Helicopter Society 67th Annual Forum*, pp. 2323-2334, 2011.

[17] Stamps Frank B., Smith Dudley and Kilmain Charles J., Multiple drive-path transmission with torque-splitting differential mechanism, *European Patent Specification EP 2084064B1*, Apr 3, 2013.

[18] Robert F. Handschuh and James J. Zakrajsek, Current research activities in drive system technology in support of the NASA rotorcraft program, *NASA Technical Memorandum 214052*, pp. 1-21, 2006.

[19] Z. Rao, C. Y. Zhou, Z. H. Deng and M. Y. Fu, Nonlinear torsional instabilities in two-stage gear systems with flexible shafts, *Int J Mech Sci*, vol. 82, pp. 60-66, 2014.

[20] Yongjun Shen, Shaopu Yang and Xiandong Liu, Nonlinear dynamics of a spur gear pair with time-varying stiffness and backlash based on incremental harmonic balance method, *Int J Mech Sci*, vol. 48, pp. 1256-1263, 2006.

[21] Krantz T. L., Majid Rashidi and Kish J. G., Split torque transmission load sharing, *NASA Technical Memorandum 105884*,

pp. 1-25, 1992.

[22] Krantz T. L. and Majid Rashidi, Vibration analysis of a split path gearbox. *In: AIAA/SAE/ASME 31st Joint Propulsion Conference*, pp. 1-14, 1995.

[23] Yang Zhen, Wang Sanmin and Fan Yesen, Nonlinear dynamic characteristics of split-torque gear transmission system, *Chin J Mech Eng*, vol. 44, pp. 52-57, 2008.

[24] Du Jiajia, Wang Sanmin and Wang Ying, Research on dynamic characteristics of the dual power path gear transmission, *Machinery*, vol.50, pp. 10-12, 2012.

[25] Zhang Ting, Li Yuxi and Wang Sanmin, Research on static load sharing of the dual power path gear transmission, *J Mech Transm*, vol. 36, pp. 14-16, 2012.

[26] Dong Hao, Fang Zongde, Wang Baobin and Du Jinfu, Load-sharing characteristics of gear train with dual power split based on deflection compatibility, *J South Chin Univ Tech*, vol.40, pp. 18-22, 2012.

[27] Dong Hao, Fang Zongde, Wang Baobin and Du Jinfu, Load sharing characteristics analysis of power split system based on deflection compatibility and clearance floating, *J Aerosp Power*, vol.28, pp.872-877, 2013.

[28] Zhao Ning, Wang Ruifeng, Jia Qingjian and Fu Bibo, Study on load sharing method for parallel shaft split torque transmission system, *J Mech Transm*, vol.37, pp. 13-16, 2013.

[29] J. V. Milanovic Smieee, C. P. N. Fu and R. R. Z. Lazarevic, Sensitivity of torsional modes and torques to uncertainty in shaft mechanical parameters, *Electr Pow Compo Sys*, vol. 29, pp.867-881, 2011.

[30] Zhu Zengbao, Zhu Rupeng, Bao Heyun and Jin G. H., Impact of run out and meshing frequency errors on dynamic load sharing for encased differential herringbone train, *J Aerosp Power*, vol.26, pp. 2601- 2609, 2011.